PHYSICAL REVIEW B **96**, 081406(R) (2017)

Parity breaking in a double atomic chain system

J. Aulbach,[1] S. C. Erwin,[2] J. Kemmer,[1] M. Bode,[1] J. Schäfer,[1] and R. Claessen[1]

[1]*Physikalisches Institut and Röntgen Center for Complex Material Systems (RCCM), Universität Würzburg, D-97074 Würzburg, Germany*

[2]*Center for Computational Materials Science, Naval Research Laboratory, Washington, DC 20375, USA*

(Received 10 July 2017; published 22 August 2017)

We use scanning tunneling microscopy to investigate the interactions between atomic chains, of two different types, formed by the adsorption of submonolayer Au onto a stepped Si surface. The first chain consists of a double row of Au atoms. The second is a single row of Si dangling bonds at the edges of the steps. The two chains are interspersed and hence each could, in principle, influence the other structurally as well as electronically. However, we find this interaction to be highly unidirectional: The Au chains modulate the Si chains, breaking their parity and lending them directionality, while the Si chains leave the Au chains unaffected.

DOI: 10.1103/PhysRevB.96.081406

Adsorption of a submonolayer of Au on a stepped Si substrate leads to highly ordered atomic wire arrays [1]. Such quasi-one-dimensional systems allow the study of unusual quantum phenomena such as Peierls instabilities [2–4], the breakdown of the canonical Fermi liquid paradigm [5,6], and low-dimensional spin interactions [7,8]. Recently, the surfaces of the so-called Si(hhk)-Au family have attracted attention due to the formation of ordered arrays of dangling bond orbitals at the exposed substrate edges [7,9–11]. The occurrence of localized edge spins is reminiscent of what has been found for graphene edges [12]. Indeed, the step edges of all known Si(hhk)-Au systems are formed by a graphitic (sp^2-hybridized) Si honeycomb chain [1]. The terrace itself always hosts an atomic Au chain which can be either a single or a double strand. Systems with wider terraces, such as Si(557)-Au and Si(775)-Au, contain an additional row of Si adatoms [1,9]. Depending on the detailed terrace composition and the resulting electron transfer, the silicon honeycomb nanoribbon situated at the step edges of the Si(hhk)-Au surfaces can be spin polarized and charge ordered [9]. This results in periodic arrays of local magnetic moments that can be considered as "spin chains" [9].

The system in focus of this Rapid Communication, Si(553)-Au, exhibits a spin chain with threefold periodicity along the one-dimensional (1D) axis. [10,11]. Specifically, every third step edge dangling bond is occupied by only one electron and hence spin polarized, while the two orbitals in between are doubly occupied and thus spin compensated [7]. The Au atoms on the terrace form a double-strand ladder, with rungs formed by Au dimers. These are tilted with alternating sign [7,13], thereby imposing a twofold periodicity along the Au chain. The electrons confined in the metallic Au chain give rise to a wiggled quasi-1D Fermi surface which reflects a small degree of coupling between the Au chains of adjacent terraces. A non-negligible two-dimensional (2D) interaction, i.e., magnetic coupling, is also predicted for the Si edge spins [7]. However, long-range magnetic ordering is impeded by a frustrated geometry, which favors a 2D spin liquid scenario [8].

The issue of interchain interactions between either the metal adatom chains or the Si chains, respectively, bears interesting implications for the temperature-dependent and thus dynamic behavior. This pertains to, e.g., the rather unexplored changes of the charge pattern in the step edge chain [3,4,14] with its distinct $\times 3$ superstructure, which upon heating to room temperature (RT) disappears completely. Instead, scanning tunneling microscopy (STM) and diffraction experiments find a $\times 1$ period [3,4]. Another example demonstrating the importance of interwire interactions is the atomic indium chains on Si(111) [15,16]. Coupling of two such chains gives rise to domain boundaries described as solitons [15], where the relative phase between the In chains induces a "chiral" character. Up to here, these couplings take place between 1D structures of the *same* type, i.e., for the metal adatom and the Si chain subsystems separately. As an evident extension of this simplified view, and with Si(553)-Au as a well-defined "two chain type" model system, the impact of mutual interaction between directly neighboring Au and Si chains with their different periodicities has yet to be examined, which is the objective of the present Rapid Communication.

Here, we employ STM to inspect the charge distribution of the Au chains on one hand, and the energetics and periodicity of the spin chains on the other hand. We arrive at an unexpected interaction hierarchy: The Si spin chain, squeezed between the Au strands, responds to its environment, as reflected in a significant energy modulation of the spin sites. The response behavior is unidirectional, i.e., the Si chains are affected by their immediate Au chain environment on both sides, but not vice versa. As a consequence, we find that the step edge spin chains are modulated with a complex sixfold periodicity. It breaks parity along the chain axis, which results in two degenerate variants of opposite directionality. The underlying heterogeneous interchain coupling thus renders this system a prime candidate for future studies of dynamic phenomena, such as melting of the spin order or the potential occurrence of coupled solitons.

For the experimental sample preparation we used n-doped (phosphorus) Si(553) substrates which were heated up to 1250 °C via direct current to remove the protective oxide layer. Au evaporation of 0.48 ML was performed while the substrate was held at a temperature of 650 °C, followed by a short postannealing at 850 °C [10,17]. STM measurements have been performed with a commercial low-temperature STM instrument from Omicron at a sample temperature of 77 K. Scanning tunneling spectroscopy (STS) spectra as well as dI/dV maps have been recorded with the lock-in technique using a modulation amplitude of 10 meV.

The discussion of our results is arranged as follows: First, we examine the periodicity of the Si step edge, finding

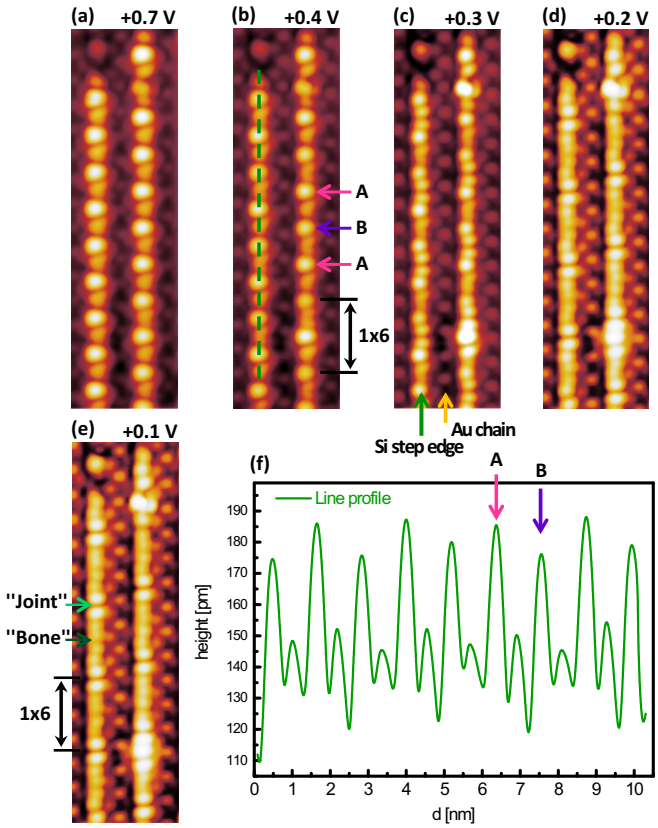

FIG. 1. (a)–(e) STM images of the unoccupied states of the Si(553)-Au surface at various tunneling biases recorded at $T = 77$ K. (f) Line profile along the Si step edge at +0.4 eV [dashed green line in (b)]. At tunneling biases of +0.3 and +0.4 V, spin sites A and B exhibit a clear intensity difference (see magenta and purple arrows as well as the line profile), leading to a sixfold modulation of the spin chain. At low tunneling bias, the Si step edge features a second $\times 6$ periodicity reflected in a bone-and-joint-like appearance of the non-spin-polarized Si atoms (see dark and light green arrows). At +0.3 V, the Si chain exhibits a superposition of both $\times 6$ intensity modulations.

two different yet undetected sixfold modulations. Then, we reveal by STS that the small intensity modulations are of an electronic nature and trace their origin back to interactions with the neighboring Au atom chains on either side. As we will see, these couplings ultimately break parity and introduce a directionality in the spin chain.

Figure 1 presents constant current STM images of unoccupied states of the Si(553)-Au surface taken at various tunneling biases. This image series allows us to identify two distinct long-range modulations of the Si step edge, which manifest at different bias values. At +0.7 V, the Si step edge—the bright chain in this image—displays the well-established $\times 3$ superstructure [3,4,10,11,18]. As already mentioned above, it is caused by *charge ordering* along the Si honeycomb chain [7,10,19], with the dangling bond of every third step edge Si atom occupied by only one electron [7]. In contrast, the dangling bonds of the other Si edge atoms in between are occupied by two electrons each, forming inactive "lone pairs" [7,9]. Consequently, only the spin-polarized Si atoms exhibit an unoccupied state as a final state for tunneling into the step edge. Energetically, it is located about +0.4 eV above the Fermi level [7,10,11,19], giving rise to the pronounced $\times 3$ superstructure visible in STM images sensitive to this state (i.e., for a tunneling bias $\geqslant +0.3$ V). However, when looking closer at the STM topography in Fig. 1(b), a small additional modulation can be discerned: Every second spin site appears brighter (site A) than the other (site B). This is best seen in the line profile displayed in Fig. 1(f) taken along the dashed green line in Fig. 1(b). The clear intensity modulation between consecutive spin sites leads to an overall *sixfold* periodicity along the Si step edge.

The second long-range modulation is observed at biases close to the Fermi level. At $U \leqslant +0.2$ V, the spin sites do not exhibit any significant tunneling density of states (DOS), hence no distinct $\times 3$ superstructure is observed. Instead, the step edge features a $\times 6$ periodic structure which is reminiscent of "bones" linked by bright "joints" [see labels in Fig. 1(c)], both formed by pairs of nonpolarized Si atoms. For an intermediate tunneling voltage, e.g., +0.3 V, the Si step edge shows a superposition of its low and high tunneling bias appearance: The bones and joints are still visible, while the two girdling spin-polarized Si atoms start to become prominent.

Before giving a detailed explanation for the bias-dependent step edge appearance, we would like to elucidate the intensity difference of consecutive spin sites in more detail. For this purpose, we have acquired dI/dV maps in the bias range of the DOS peak characteristic for the spin-polarized step edge atoms [see Fig. 2(a)]. One can clearly identify a localized DOS intensity with $\times 3$ spacing in all dI/dV maps, although their respective intensities vary with the set-point voltage. For a low tunneling bias (0.20–0.30 V), spin site A appears brighter than site B. With increasing bias both sites first become indistinguishable and then reverse their behavior, with site B becoming more intense than A for bias voltages $\geqslant$0.45 V. These observations clearly indicate that the unequal appearance of spin sites A and B in the topography images of Fig. 1 originates from a relative energy difference between their associated DOS peaks. This is indeed confirmed by a direct measurement of the local STS spectra, as shown in Fig. 2(b). The measured energy shift between the DOS peaks of both spin sites amounts to about 20 meV. Both the dI/dV maps as well as the tunneling spectra clearly demonstrate that the inequivalence between adjacent spin sites is of an electronic nature rather than a topographic effect. Further support for the absence of any distinct structural motif with $\times 6$ periodicity is given by the absence of any $\times 6$ features in the electron diffraction pattern reported earlier [8].

In the following, we will discuss the origin of the energy-shifted DOS. For this purpose, we turn to the second chain type of the system, the Au chain. Importantly, the Au dimers which reside on the terraces of Si(553)-Au [7,13] are slightly tilted in alternating fashion from rung to rung along the Au ladder. This tilted dimer structure is not directly resolved in STM images [10], but circular charge clouds with $\times 2$ periodicity are observed [see the low bias images of Figs. 1 or 3(a)]. However, this does not question the established structural model for Si(553)-Au [7,13], but serves as additional support: Density functional theory (DFT) simulations of the (energy-integrated) local DOS distribution reveal a DOS accumulation in between the closer Au atoms of each strand of the $\times 2$ periodic Au

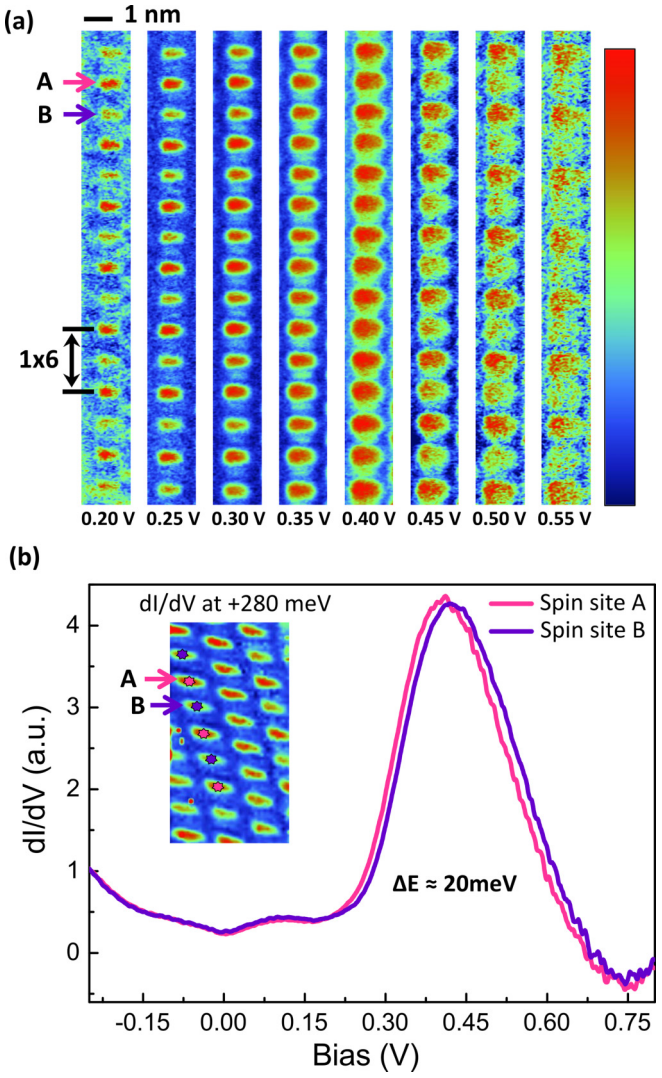

FIG. 2. (a) dI/dV maps of a Si step edge spin chain at various tunneling biases. At low tunneling bias, a clear DOS imbalance between neighboring spin sites is observed. This imbalance inverts for high tunneling bias, which provides clear evidence for its electronic nature. (b) Local tunneling spectroscopy on different spin sites. Inset: dI/dV map at 280 meV. The magenta and purple dI/dV curves represent spectra taken at spin sites A and B, respectively, as marked in the inset. The dI/dV curves of spin sites A and B are found to be shifted by 20 mV with respect to each other.

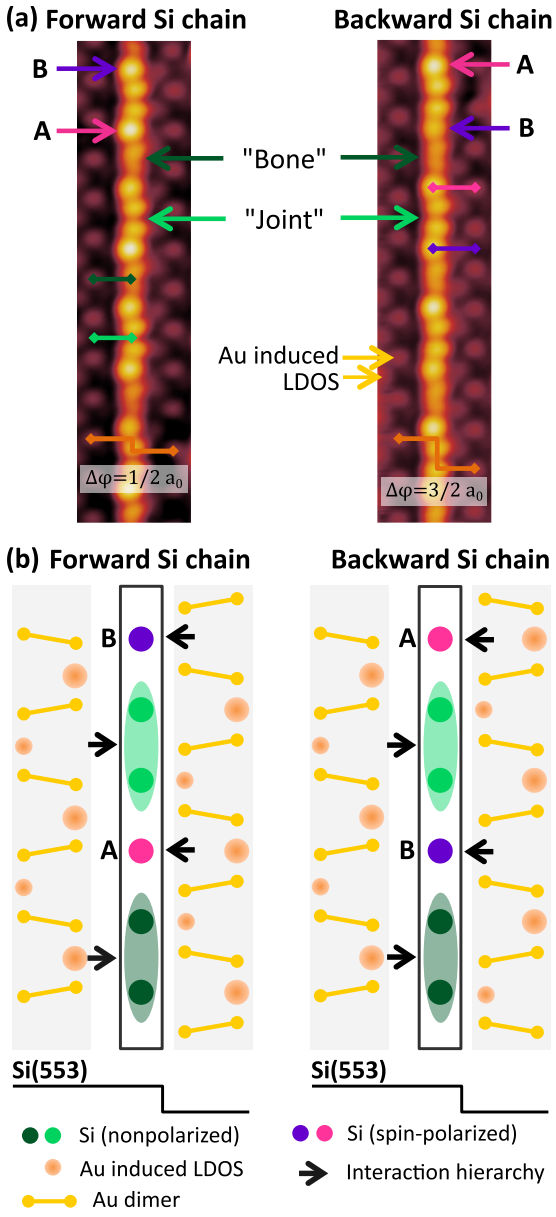

FIG. 3. (a) Constant current STM images taken at +0.3 V of two Si spin chains with different directionalities. The forward Si chain (left image) is characterized by a brighter spin site A (B) located below (above) the joint feature, respectively (see purple and magenta arrows).The backward Si chain (right image) shows the reverse sequence. Magenta and purple markers indicate the fixed phase relation between the Au charge clouds of the right-sided Au chain and the spin sites A and B. Green markers visualize the fixed phase relation of the bone-and-joint features to the left-sided Au chain. (b) Schematic illustration of the interaction between Au chains and enclosed Si step edge. The Au chains induce a parity breaking of the enclosed step edge. The directionality of the spin chain is determined by the phase relation of the surrounding Au chains.

double chain, which is in perfect agreement with the charge accumulation observed in the low bias STM images [10]. Thus, the charge clouds do not only represent the tilted rungs of the Au ladder but also allow us to inspect the phase relation of neighboring Au chains, which is of importance for the subsequent arguments.

Figure 3(a) provides STM images taken at +0.3 V, the bias value sensitive to both the bone-and-joint structure formed by the nonpolarized Si atoms as well as the inequivalent DOS of spin sites A and B. Notably, these closeups of the Si chains reveal a finely modulated pattern, rendering the atoms with different intensities. As a key characteristic, the atoms A and B as well as the joint and bone segments (as marked in the images) do not carry the same intensity. This is in contrast to the simple picture expected for isolated Si chains with a dangling bond on every third site, which would imply a mirror plane perpendicular to the chain direction. This is obviously lacking, i.e., the parity of the step edge is broken. Instead, two different step edge variants occur which exhibit opposite directionality. The two variants are denoted as the “forward”

and "backward" Si chain, and are directional in that they cannot be mapped onto each other by translation.

More specifically, the forward chain in the image on the left of Fig. 3(a) is characterized by the following repeat sequence (from top to bottom): spin site B–joint segment–spin site A–bone segment. In contrast, the backward chain in the image on the right displays the reversed sequence, encountering first site B and then site A.

We now turn to the origin of the parity breaking and the determining factors of the step edge direction. Here, the neighboring Au chains and their phase relation play a primary role. A phase shift of $\Delta\varphi = \frac{1}{2}a_0$, where a_0 is the distance between two Si atoms along the step edge, results in a forward Si chain, and $\Delta\varphi = \frac{3}{2}a_0$ leads to a backward Si step edge [see orange markers in Fig. 3(a)]. The background of this simple relationship can be understood by a close inspection of the phase shifts between the spin chain features and the adjacent Au chains. The position of the inequivalent spin sites is determined by the Au chain of the neighboring *downhill* terrace (and notably not the same-level terrace), i.e., the Au chains to the right of the spin chains pictured in Fig. 3(a): The bright spin site A is always located next to the charge cloud of the adjacent Au chain, while the darker spin site B always sits between the Au charge clouds [see magenta and purple markers in Fig. 3(a)]. The inequivalence of the nonpolarized Si atoms, i.e., their joint and bone appearance, is also identified to be Au chain induced. Contrary to the spin-polarized Si atoms, the nonpolarized Si atoms are influenced by the Au chain located on the *same* terrace as inferred by their strict phase relation: The joint (bone) structures always appear between (next to) charge clouds of the left-side Au chain, as indicated by the light and dark green markers in Fig. 3(a).

Regarding their respective transverse phase correlations, both chain subsystems behave fundamentally different: The spin chains exhibit an exceptionally strong interwire coupling which results in a fixed phase relation between neighboring spin chains [8]. On the contrary, the Au chains do not show any fixed phase correlation. Instead, the phase between adjacent Au chains switches randomly between $\frac{1}{2}a_0$ and $\frac{3}{2}a_0$. This becomes evident from $\times 2$ streaks instead of $\times 2$ spots in the diffraction pattern [3,8]. As a consequence, no preference for one of the two spin chain variants exists but forward and backward spin chains are evenly distributed over the Si(553)-Au surface.

Figure 3(b) visualizes the experimental observation from the structural point of view. The tilting of the Au dimers, i.e., the local charge distribution in the Au chain, influences the neighboring spin chain elements and lifts the degeneracy of their DOS, as indicated by the color coding of the step edge and the arrows. The Au chain on the right-hand side of the spin chain (neighboring terrace) affects the *spin sites* and the Au chain on the left (same terrace) the *nonpolarized* Si atoms.

To get deeper insight into the interaction mechanism, we recall the periodicities of both chain types. Surprisingly, the Au chain does not show any indication of a $\times 6$ superstructure [see Fig. 3(a)]. Thus, the spin chain and its distinct $\times 3$ periodicity do not affect the Au chain, while the Au strand imprints its $\times 2$ periodicity on the Si step edge, leading to the long-ranged $\times 6$ modulation. Therefore, we infer that the net result of the interaction is unilateral, i.e., characterized by a hierarchy, where the Au chains affect the step edges but not vice versa.

In conclusion, the atomic-scale inspection of the multiple ordered superstructures that coexist in the Si(553)-Au system at low temperatures has unveiled a surprising level of detail and complexity. While the $\times 2$ periodicity of the Au strands and the $\times 3$ periodicity of Si step edge has long since been known, our tunneling spectroscopy analysis now reveals a long-ranged *sixfold* superstructure in addition. This can be explained by a subtle interaction between the Au and Si chains. Specifically, nonpolarized Si atoms respond to the Au strand on the same terrace, while spin sites follow the neighboring Au chain on the adjacent downhill terrace, thereby displaying overall a hierarchical dependency of this modulation on the metal adatom structure. The net result is a *parity breaking* of the step edge in two variants.

These findings extend the previous reports of the fundamental ($\times 2$, $\times 3$) periodicities, described in a global Peierls-type charge density wave picture, without referring to the dangling bond spins [3,4,18]. From those studies, it was nonetheless established that the dominant periodicity seen in STM (threefold on the Si step edge) vanishes in favor of a $\times 1$ periodicity at RT, while details at intermediate temperatures (such as spin hopping modeled in Ref. [14]) are not elucidated experimentally until now. The results presented here provide motivation to look into this phenomenon from the point of view of laterally interacting 1D spin chains. In this context, occasional phase shifts have been noted in the Si step edge chain, and speculation was made about the applicability of a solitonlike description [4,18]. Recently, evidence for solitons has been reported for In chains on planar Si(111). There, two In-based Peierls chains couple with each other, and, depending on their relative alignment, form a chiral soliton [15,20]. In the light of our above results for Si(553)-Au, which is distinguished from In-Si by the added step edge Si chain, a collective behavior of the Au strand and Si chain becomes manifest, leading to the yet unanswered question whether "coupled solitons" as a joint excitation may exist in such low-dimensional systems.

We acknowledge fruitful discussions with F. F. Assaad, M. Greiter, and R. Thomale. This work was supported by Deutsche Forschungsgemeinschaft (through SFB 1170 "ToCoTronics" and FOR 1700) and the Office of Naval Research through the Naval Research Laboratory's Basic Research Program (SCE).

[1] J. N. Crain, J. L. McChesney, F. Zheng, M. C. Gallagher, P. C. Snijders, M. Bissen, C. Gundelach, S. C. Erwin, and F. J. Himpsel, Phys. Rev. B **69**, 125401 (2004).

[2] M. D. Johannes and I. I. Mazin, Phys. Rev. B **77**, 165135 (2008).

[3] J. R. Ahn, P. G. Kang, K. D. Ryang, and H. W. Yeom, Phys. Rev. Lett. **95**, 196402 (2005).

[4] P. C. Snijders, S. Rogge, and H. H. Weitering, Phys. Rev. Lett. **96**, 076801 (2006).

[5] F. D. M. Haldane, J. Phys. C **14**, 2585 (1981).

[6] P. Segovia, D. Purdie, M. Hengsberger, and Y. Baer, Nature (London) **402**, 504 (1999).
[7] S. C. Erwin and F. Himpsel, Nat. Commun. **1**, 58 (2010).
[8] B. Hafke, T. Frigge, T. Witte, B. Krenzer, J. Aulbach, J. Schäfer, R. Claessen, S. C. Erwin, and M. H.-V. Hoegen, Phys. Rev. B **94**, 161403(R) (2016).
[9] J. Aulbach, S. C. Erwin, R. Claessen, and J. Schaefer, Nano Lett. **16**, 2698 (2016).
[10] J. Aulbach, J. Schäfer, S. C. Erwin, S. Meyer, C. Loho, J. Settelein, and R. Claessen, Phys. Rev. Lett. **111**, 137203 (2013).
[11] I. Song, J. S. Goh, S.-H. Lee, S. W. Jung, J. S. Shin, H. Yamane, N. Kosugi, and H. W. Yeom, ACS Nano **9**, 10621 (2015).
[12] G. Z. Magda, X. Jin, I. Hagymasi, P. Vancso, Z. Osvath, P. Nemes-Incze, C. Hwang, L. P. Biro, and L. Tapaszto, Nature (London) **514**, 608 (2014).
[13] M. Krawiec, Phys. Rev. B **81**, 115436 (2010).
[14] S. C. Erwin and P. C. Snijders, Phys. Rev. B **87**, 235316 (2013).
[15] S. Cheon, T.-H. Kim, S.-H. Lee, and H. W. Yeom, Science **350**, 182 (2015).
[16] H. W. Yeom, S. Takeda, E. Rotenberg, I. Matsuda, K. Horikoshi, J. Schaefer, C. M. Lee, S. D. Kevan, T. Ohta, T. Nagao, and S. Hasegawa, Phys. Rev. Lett. **82**, 4898 (1999).
[17] J. N. Crain, A. Kirakosian, K. N. Altmann, C. Bromberger, S. C. Erwin, J. L. McChesney, J.-L. Lin, and F. J. Himpsel, Phys. Rev. Lett. **90**, 176805 (2003).
[18] J. S. Shin, K.-D. Ryang, and H. W. Yeom, Phys. Rev. B **85**, 073401 (2012).
[19] P. C. Snijders, P. S. Johnson, N. P. Guisinger, S. C. Erwin, and F. J. Himpsel, New J. Phys. **14**, 103004 (2012).
[20] T.-H. Kim, S. Cheon, and H. W. Yeom, Nat. Phys. **13**, 444 (2017).